Biosensors and Bioelectronics 154 (2020) 112066

Contents lists available at ScienceDirect

Biosensors and Bioelectronics

journal homepage: http://www.elsevier.com/locate/bios

High-sensitive and multiplex biosensing assay of NSCLC-derived exosomes *via* different recognition sites based on SPRi array

Yunpeng Fan [a,1], Xiaolei Duan [a,1], Min Zhao [a], Xiaotong Wei [a], Jiangling Wu [a], Wenqin Chen [a], Ping Liu [b], Wei Cheng [c], Quan Cheng [d], Shijia Ding [a,*]

[a] Key Laboratory of Clinical Laboratory Diagnostics (Ministry of Education), College of Laboratory Medicine, Chongqing Medical University, Chongqing, 400016, China
[b] Bioscience (Tianjin) Diagnostic Technology CO., LTD, Tianjin, 300000, China
[c] The Center for Clinical Molecular Medical Detection, The First Affiliated Hospital of Chongqing Medical University, Chongqing, 400016, China
[d] Department of Chemistry, University of California, Riverside, 92521, CA, USA

ARTICLE INFO

Keywords:
Exosomes
Non-small cell lung cancer
Surface plasmon resonance imaging
Functionalized gold nanoparticles
Biosensing assay

ABSTRACT

Non-small cell lung cancer (NSCLC) have been reported to secret a high concentration of exosomes into blood circulatory system, which is one of sensitive and non-invasive biomarkers for NSCLC's early-stage diagnosis. But it is still lack of feasible and accurate methods to analyze the different NSCLC cells-derived exosomes. Herein, we built a SPRi biosensing assay for high-sensitive and multiplex characterizations of NSCLC-derived exosomes by bioaffinity interactions of antibodies and different recognition sites. By this way, the exosomes derived from normal lung and NSCLC cells can be effectively distinguished through precise identification of the exosomal protein pattern. And the multiplex characterizations of NSCLC-related exosomes are also achieved by anti-CD63, anti-EGFR and anti-EpCAM modified SPRi array. The limit of detection (LOD) of this SPRi-based biosensor approaches to the level of 10^4 particles/μL with the help of functionalized gold nanoparticles. Besides, the developed biosensing assay was successfully applied in the determination of exosomes purified from clinical plasma samples. This SPRi biosensing strategy might offer a potential alternative for massive high-throughput screening for NSCLC in clinical specimens.

1. Introduction

Lung cancer accounts for ~13% in all cancer cases in worldwide, which remains the highest mortality of all cancer types with an estimated 1.6 million deaths in each year (Bray et al., 2018). According to the World Health Organization (WHO) in 2015, approximately 85% of patients of lung cancers have a group of pathological subtypes: NSCLC, and the 5-year survival rate of NSCLC patients is as low as 10–15% (Herbst et al., 2018). The main reason of NSCLC with such poor prognosis is due to the delay in detection of this tumor, and NSCLC patients are usually diagnosed in an advanced disease stage (Abbosh et al., 2017). Nevertheless, we clinically assess the histological grade of NSCLC by tumor cell differentiation, which lacks surveillance of early-stage symptoms. Therein, it is urgent to find sensitive and non-invasive biomarkers, such as microRNA, nucleic acids (Navab et al., 2011), proteins (Aguiar et al., 2016), exosomes (Taverna et al., 2016) and so on, for NSCLC's screening and early diagnosis.

Exosomes, as emerging biomarkers in liquid biopsy, are disk-like vesicles with 30–150 nm in diameter and secreted by most types of mammalian cells (Van et al., 2018). They serve as potent mediators of intercellular communication and have essential roles in tumorigenesis. As appearing in the early stages of carcinoma, exosomes transfer selected proteins, lipids, nucleic acids, and glycoconjugates, from parental to recipient cells (Boriachek et al., 2018). Currently, growing evidence has proposed that stem cells of NSCLC proliferate other tumor cell types e.g., A549, H460, and H1299. These cell lines secrete respective exosomes, which carry different amounts of multitudinous proteins such as CD63, EGFR, EpCAM and so on (Ho et al., 2007). Plenty of these proteins regulate the malignant biological activity and are displayed on exosomal membrane, resulting in different amounts of surface phenotype (Wu et al., 2012). Under this circumstance, probing the subtle variations of surface phenotype among these exosomes cannot only predict metabolic stage of cells but also distinguish parent cell types of NSCLC. This information is able to offer help to the NSCLC's diagnosis

* Corresponding author.
E-mail address: dingshijia@cqmu.edu.cn (S. Ding).
[1] These authors contributed equally to this work.

https://doi.org/10.1016/j.bios.2020.112066
Received 14 December 2019; Received in revised form 19 January 2020; Accepted 27 January 2020
Available online 28 January 2020

and therapy. Nevertheless, it poses a great challenge because of the lack of feasible and accurate profiling methods.

In recent years, considerable researches have revealed that tumor cells secret higher concentration of exosomes into peripheral blood (Lobb et al., 2017; Wang et al., 2018), which carry tumor specific molecules. Thereby, probing specific tumor-derived exosomes in peripheral blood becomes an emerging paradigm in clinical diagnosis of cancers. However, conventional methods used for analysis of tumor-derived exosomes, such as Western blot, ELISA and mass spectrometry, suffer from lengthy processes and labor, thus limiting their clinical applications. To date, there are some novel protocols for the determination of tumor-derived exosomes (Ferhan et al., 2018; Shao et al., 2018). For example, previous studies have reported surface-enhanced Raman scattering (SERS) immunoassay to specifically detect pancreatic and breast tumor-derived exosomes with a high sensitivity (Li et al., 2018; Kwizera et al., 2018). These SERS-based immunoassays are labeled by Raman reporter. Besides, Jiang et al. have adopted aptamer/AuNP sensor to profile four kinds of tumor-derived exosomes by surface proteins based on colorimetric method (Jiang et al., 2017). But, the sensitivity of this protocol is poor. In terms of NSCLC, sensitive and specific detection tumor-derived exosomes is under way. He and her colleagues have developed microfluidic approach to isolate and analyze the exosomes from NSCLC cells, by which they were able to assess the phenotyping and the phosphorylation levels of exosomes (He et al., 2014). Additionally, Yu et al. have designed fluorophore-labeled magnetic beads based on aptamer specific to CD63 to determine the concentration of exosomes from NSCLC cells (Yu et al., 2019). Their method is able to detect exosomes as low as 1.0×10^5 particles/μL. However, the aforesaid two processes for analysis of NSCLC-derived exosomes are complicated and need fluorescent tags. Therein, the development of innovative detection method for NSCLC-derived exosomes is highly desirable, which requires high sensitivity, non-labeling and high-throughput screening.

To explore this possibility, we will aim to determine the populations and subtypes of NSCLC-derived exosomes by SPRi biosensing platform, owing to its advantages of high sensitivity, non-labeling, point-of-care and multiplex detection in clinical applications (Scarano et al., 2010; DiNoto et al., 2016; Thakur et al., 2017). Accordingly, it can acquire imperative information about the parent cell types of NSCLC. To further improve the sensitivity, plasmonic nanoparticles are widely adopted to enhance SPRi signal because of their inhere advantages, such as higher refractive index, easy preparation and good biocompatibility (Lyon et al., 1998; Lv et al., 2018; Zeng et al., 2019). Under these considerations, we have constructed a SPRi biosensor for high-sensitive and multiplex characterization of NSCLC-derived exosomes by bioaffinity interactions of antibodies and different recognition sites, as shown in Scheme 1. First of all, exosomes obtained by centrifugation from different NSCLC cell culture supernatants are temporally injected into three channels in a flow chamber. The exosomes of different subtypes can be captured by each antibody-modified SPRi chip, respectively. These antibodies aim at different surface phenotype, e.g., CD63, EGFR and EpCAM, on the exosomes. Then, the SPRi signal primarily has a response, due to binding of NSCLC-derived exosomes and antibodies. To more accurately determine the populations of NSCLC-derived exosomes, antibody-functionalized gold nanoparticles (AuNPs) are injected into the flow chamber to form sandwich structures of antibodies/exosome/AuNPs hybrid, leading to amplification of SPRi signal. Through this protocol, we try to monitor the populations and subtypes of NSCLC-derived exosomes in the plasma of lung cancer patients. What's more, the parent cell types of NSCLC-derived exosomes are successfully identified. Consequently, this kind of biosensing method allows for screening of several types of NSCLC among high-risk individuals from a single measurement, making it widely and economically accessible for clinical use.

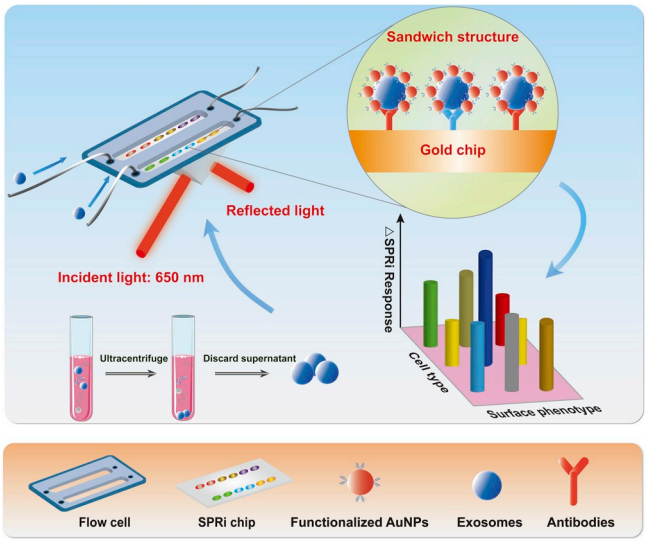

Scheme 1. Working principle of plasmonic AuNPs-enhanced SPRi biosensor for multiplex analysis of NSCLC-derived exosomes *via* different recognition sites.

2. Experimental section

2.1. Materials and reagents

Phosphate buffer saline (PBS) and bovine serum albumin (BSA) were obtained from Thermo Fisher Scientific (Wilmington, USA). Dulbecco's modified eagle medium (DMEM) and fetal bovine serum (FBS) were purchased from Gibco (Shanghai, China). Antibodies such as anti-CD63 TS63 and anti-CD9 MEM-61 monoclonal antibodies were all supplied by Abcam (MA, USA); anti-EGFR D260292 polyclonal antibody were obtained from Sangon (Shanghai, China). Both of anti-EpCAM bs-0593R and anti-CD81 bs-6934R polyclonal antibody were purchased from Bioss (Beijing, China). HRP anti-mouse A0216 and rabbit A0208 IgG were from Beyotime (Jiangsu, China). All of these antibodies in the solutions contained 0.1% (w/v) bovine serum albumin (BSA). $HAuCl_4{\cdot}4H_2O$ was purchased from Sinopharm Chem Co., Ltd (Shanghai, China). Trisodium citrate was provided by Sigma-Aldrich Chemical Co., Ltd (St. Louis, MO, U.S.A.). The other reagents in experiment were of analytical grade without any purification. Ultrapure water by Milli-Q gradient ultrapure water system (Millipore, MA) was used for preparing all aqueous solutions.

2.2. Apparatus

A SPRi platform and sensor chips with gold array were home-built. This platform has three separate channels with volume of 50 μL per channel for temporally detecting different NSCLC-derived exosomes. 2 nm thick of chromium was fabricated on the SPRi chip as adhesion layers, and then a 46 nm thick gold layer was deposited on each layer *via* e-beam evaporation. To stimulate the surface plasmon resonance on the SPRi chip, an emitting diode (LED, 650 nm) was used as optical source. A sheet polarizer ensured *p*-polarized light for SPRi measurement. The matching liquid ($n = 1.616$) was mediated between the sensor chip and prism (heavy flint glass), avoiding the influence of air. A cooled 12-bit CCD camera (Retiga 1300 from QImaging) with a resolution of 1.3 MP (1280 × 1024 pixels) and 6.7 μm × 6.7 μm pixel size was employed for capturing the images in region of interest. All sensorgrams were evaluated by a lab-developed program written in LabVIEW. Transmission electron microscopic (TEM) measurements were carried out on an H-7500 transmission electron microscope (Hitachi, Japan). Nanoparticles tracking analysis (NTA) was performed on a ZetaView-Nanoparticle tracking analyzer (Particle Metrix, Germany). The SDS-PAGE and

image analysis were acquired with electrophoresis analyzer and ChemDoc XRS (Bio-Rad, USA). UV–visible spectrum was obtained on a UV-2550 spectrophotometer (Shimadzu, Japan).

2.3. Cell culture

The human NSCLC cell lines (A549, H460 and H1299) and normal lung cell (BEAS-2B) were obtained from the American Type Culture Collection (Rockville, MD, USA). All of these cells were cultured in DMEM supplemented with 10% FBS, 1% penicillin and streptomycin at 37 °C in a humidified atmosphere containing 5% CO_2. The cells were divided every 2–3 days under sterile conditions. To reduce interference from FBS, cells (1.37×10^8 cells) were washed twice with PBS and cultured in serum-free medium (100 mL DMEM without FBS) for 48 h prior to isolation of exosomes.

2.4. Isolation of exosomes

First of all, cell culture supernatant was ultracentrifuged (10,000×*g*, 30 min) to remove intact cells, cell debris, and large microvesicles. In this study, all centrifugation performances were carried out at 4 °C unless mentioned. The supernatant was collected and then centrifuged (100,000×*g*, 70 min) to isolate NSCLC-derived exosomes. The exosomes were washed in a large volume of PBS to eliminate protein impurity, and then centrifuged again. These nanoscale vesicles were resuspended in 100 μL PBS and stored at −80 °C prior to use. To extract exosomes from human plasma, differential centrifugation was employed. 1.5 mL plasma was diluted with PBS and centrifuged (12,000×*g*, 45 min). Then the supernatant was collected in ultracentrifuge tubes and centrifuged (110,000×*g*, 2 h). After pouring off the supernatant, the remaining exosomes was resuspended in 8 mL PBS solution and filtered by 0.22 μm filters for removing nanoscale impurity. The filtrate was centrifuged (110,000×*g*, 70 min, 4 °C) to eliminate protein impurity for twice. Finally, 100 μL PBS was used to resuspend exosomes in precipitate and the resuspension was stored at −80 °C before further use. NTA was carried out to determine the concentration and size distribution of these NSCLC-derived exosomes (Fig. S3). For every SPRi measurement, ~2.5 μL exosomes from suspension was diluted with 130 μL of PBS solution and injected into the channel of flow chamber. Human plasma used in this study was obtained from the First Affiliated Hospital of Chongqing Medical University. The study was approved by the ethic committee of the First Affiliated Hospital of Chongqing Medical University.

2.5. Preparation of antibody-functionalized AuNPs

The AuNPs were synthesized by a reported method with minor modifications (Maltez-da Costa et al., 2012). Briefly, a total of 50 mL of 0.01% $HAuCl_4{\cdot}4H_2O$ was heated under vigorous stirring, and 1.2 mL of 1% trisodium citrate was dropwise added to the solution when the temperature reached 98 °C. Then, the mixture turned deep red and was cooled down under stirring to form the anticipative gold nanoparticles. Subsequently, 1 mL of as-prepared AuNPs suspension was mixed with 100 μL of 100 μg/mL anti-CD63 antibody solution at 25 °C under gentle stirring for 20 min. The antibody modified AuNPs was incubated in 5% BSA at 25 °C for 20 min to block the active sites and centrifuged for twice. Finally, the AuNPs/anti-CD63 conjugates were resuspended in PBS and stored at 4 °C prior to use. The prepared bare AuNPs and functionalized AuNPs were characterized by UV–vis spectroscopy and TEM (see Fig. S1).

2.6. Fabrication of antibodies microarray chip

The antibodies were immobilized on SPRi chip as previously described elsewhere (Zhu et al., 2014). The gold chip surface was firstly cleaned with fresh piranha solution (70% H_2SO_4, 30% H_2O_2) for 10 min to eliminate the adsorbed organic impurities, following rinsed thoroughly with ultrapure water and dried under nitrogen. Anti-CD63, anti-CD81, anti-EGFR and anti-EpCAM antibodies were diluted to a final concentration of 50 μg/mL with PBS, and anti-rabbit IgG was used as a negative control in this study. Each antibody was printed on four spots of the chip. The chip was incubated in 80% humidity at 4 °C overnight before rinse by 0.1 × PBS and ultrapure water, respectively. Then the chip was incubated in 1% (w/v) BSA for 2 h to block active sites and washed by 0.1 × PBS and ultrapure water. After blocking, the SPRi chip was dried by nitrogen.

2.7. SPRi measurement

For each SPRi measurement, PBS was initially injected into three channels of flow cell with a constant rate of 10 μL/min at 25 °C till the sensorgram reached a steady state. Then the exosomes and functionalized AuNPs were successively injected at rate of 8 μL/min to form antibodies/exosome/AuNPs hybrid on chip surfaces. A CCD was employed to detect the reflected light and transduce signal to image at the specular angle (Fig. S2). After measurement, the chip surface was regenerated with 50 mM NaOH at 20 μL/min for 2 min. The sensor chip could be regenerated 3 times while the SPR response only decreased less than 20%, suggesting the same sensor chip could be reused 3 times at least. Selected antibody-grafted regions in the SPR images were analyzed, and the average reflectivity variations of the chosen areas were plotted as a function of time. In all SPRi experiments, three replicate tests were implemented, and the average value was calculated.

3. Results and discussion

3.1. Characterization of purified exosomes

For simplicity, we refer the isolated particles by centrifugation as “exosomes”, although the isolated fraction includes unexpected ingredients. First of all, the size and morphology of NSCLC-derived exosomes (from A549 cells) were characterized by TEM measurements. We can clearly observe a typical “cup-shaped” vesicle adhere to the substrate from Fig. 1A and its diameter is ~80 nm, agreeing with what Liu et al. observed (Liu et al., 2017). The majority of these isolated exosomes remains intact. To evaluate size distribution of exosomes, NTA measurements were performed. The modal size of this kind of NSCLC cell-derived exosomes is ~80 nm as shown in Fig. 1B, corresponding to result of TEM, which has similarity to the previous reported (He et al., 2014). We also carried out Western blot to biochemically characterize the lysates of A549 cells and their derived exosomes. As shown in Fig. 1C, the proteins CD9, CD63 and CD81 are enriched in both of A549 cells and their derived exosomes. These results suggested that exosomes could be successfully obtained for further experiments. Additionally, NSCLC cell-derived exosomes almost contain members of the tetraspanin family such as CD9, CD63 and CD81, including H460 and H1299 derived-exosomes (Wang et al., 2018; Sandfeld-Paulsen et al., 2016).

3.2. Feasibility of multiplex assays of exosomes via different recognition sites

To estimate the feasibility of the developed SPRi biosensor for detection of NSCLC-related exosomes *via* different recognition sites, two typical tetraspanins (CD63 and CD81) were chosen as targets to capture A549 cell-derived exosomes. As shown in Fig. 2, the anti-rabbit IgG (curve 1) as negative control generated a negligible SPRi signal response when 130 μL of 50×10^4 particles/μL A549 cell-derived exosomes simultaneously entered into both channels of flow chamber, indicating nonspecific bioaffinity on gold chips. Upon modification of specific antibodies (anti-CD63 or anti-CD81) on gold chips, distinct level of SPRi signal responses were observed when the same amounts of A549 cell-derived exosomes was added (curve 2), demonstrating these exosomes were successfully anchored. Moreover, the difference between the SPRi

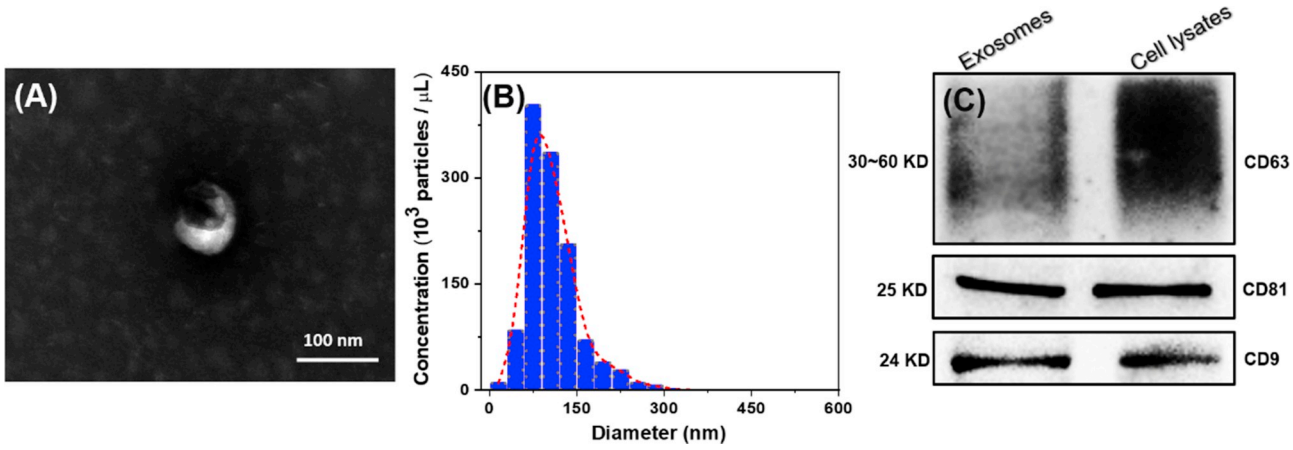

Fig. 1. Characterization of exosomes from A549 cells: (A) TEM image of exosomes obtained. Scale bars: 100 nm; (B) Representative size histogram of the exosomes by NTA demonstrates their size distribution. Red dot plot is log-normal fitting ($R^2 > 0.96$); (C) Western blot of proteins in the exosomes. Cell lysates was set as a positive control. (For interpretation of the references to color in this figure legend, the reader is referred to the Web version of this article.)

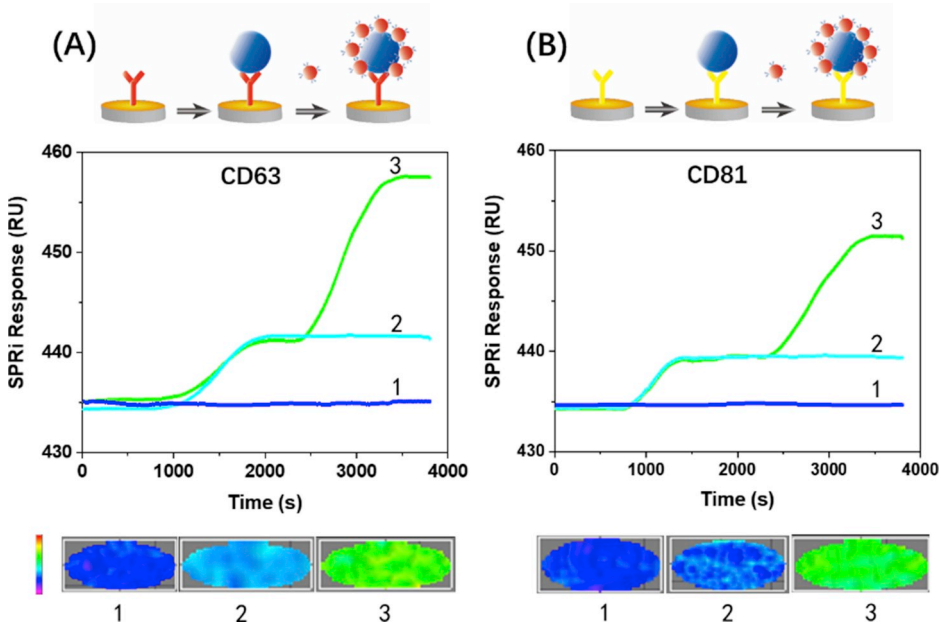

Fig. 2. SPRi sensorgrams for multiplex detection of A549 cell-derived exosomes by the recognition sites of CD63 and CD81. Curve 1, 2 and 3 represent negative control, addition of exosomes, and exosomes/functionalized AuNPs, respectively. The 3D SPRi images in the bottom panel demonstrate the intensity of reflected light after each operation.

response of anti-CD63 and anti-CD81 suggested a better performance of CD63 than CD81 in capturing exosomes (Oliveira-Rodriguez et al., 2016). Subsequently, anti-CD63 functionalized AuNPs were injected to flow cell to form sandwich structures of antibodies/exosome/AuNPs hybrid, which caused remarkable increases of SPRi signal responses (curve 3) due to enhanced effects of AuNPs (Lyon et al., 1998). Anti-rabbit IgG/AuNPs was used as control to confirm the specificity of anti-CD63 functionalized AuNPs in targeting exosomes (Fig. S4). On the other hand, final intensity of reflected light was recorded by CCD during each operation and then analyzed by software ImageJ to obtain 3D SPRi images as shown in the bottom panel of Fig. 2, agreeing with the sensorgrams. Therein, A549 cell-derived exosomes can be captured by anti-CD63 or anti-CD81 modified gold chips and AuNPs are able to significantly amplify the SPRi signal response. These results demonstrated the possibility of our SPRi biosensor for multiplex characterization of exosomes *via* different recognition sites.

3.3. Sensitive detection of NSCLC-derived exosomes by SPRi biosensor

Under the optimum conditions (see Fig. S5), we added different concentrations of A549 cell-derived exosomes into the flow cell. These exosomes were anchored based on the bioaffinity between anti-CD63 and CD63 proteins on the surface of them. In the same way, AuNPs were used to amplify the SPRi signal during the experimental. As shown in Fig. 3a, it is obvious that SPRi signal response gradually increased with concentration from 3.125×10^4 to 100×10^4 particles/μL. Then, we counted the SPRi signal as function of the exosomes concentration. It was found that favorable linear relationship between the SPRi signal and exosomes concentration. The linear fitting equation was $\triangle I = 0.507C - 1.20$ ($R^2 = 0.98$, where $\triangle I$ is the difference of SPRi response before and after each operation, and C is the concentration of exosomes). Notably, limit of detection (LOD) towards NSCLC-derived exosomes by our constructed SPRi biosensor was estimated to be 2.37×10^4 particles/μL. By contrast, this sensitivity of SPRi biosensor can approach to the similar

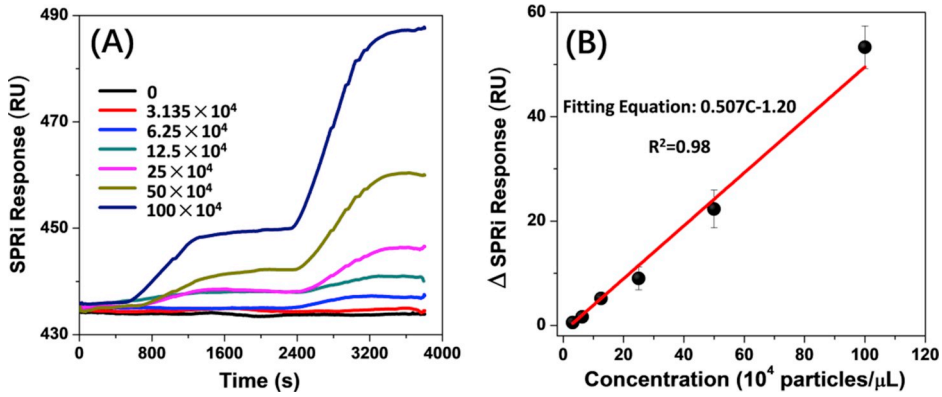

Fig. 3. (A) SPRi sensorgrams for detection of A549 cell-derived exosomes in the concentrations ranging from 0 to 100 × 10^4 particles/μL. (B) SPRi signal response functions as concentrations of A549 cell-derived exosomes by the designed SPRi platform. In this study, all data expressed as mean ± standard variation (n = 3).

level of previously reported SPRi methods (Table S1) (Zhu et al., 2014; Gool et al., 2017; Picciolini et al., 2018), attributing to excellent bio-affinity of anti-CD63 and CD63 proteins, and AuNPs' enhanced effects.

3.4. Distinguish of normal lung and NSCLC cell-derived exosomes by multiple recognition sites

To confirm the validity of recognition sites on NSCLC cell-derived exosomes, lysates of A549 cell-derived exosomes were characterized by Western blot. As reference, normal lung cell (BEAS-2B)-derived exosomes were also evaluated by the same way. In Fig. 4A and S6, it seems that expression of EGFR is higher than CD63 and EpCAM in A549 cell-derived exosomes; while these three kinds of proteins are enriched in A549 cell-derived exosomes than those from BEAS-2B cells. The results are consistent with previously reported (Clark et al., 2016). Thereby, we consider the three proteins as different recognition sites to detect NSCLC cell-derived exosomes by SPRi biosensor. Afterwards, we immobilized antibodies anti-CD63, anti-EpCAM and anti-EGFR on the SPRi chip to specifically screen exosomes from A549 and BEAS-2B cells, respectively. Fig. 4B demonstrates that the SPRi responses were obviously distinct *via* different recognition sites of CD63, EpCAM and EGFR in the two exosomes. Taking A549 cell-derived exosomes for example, SPRi signal based on CD63 sites seemed the same as that of EpCAM; while, the SPRi signal by EGFR sites had strongest response among the three proteins, illustrating a high expression of EGFR than CD63 and EpCAM on the NSCLC cell-derived exosomes. This is one of the important characteristics of NSCLC cells and the overexpression of EGFR on membrane of exosomes promotes abnormal growth and division of parent NSCLC cells (Yang et al., 2015). Compared with A549 cell-derived exosomes, the exosomes from BEAS-2B cells has weaker SPRi signal response by the three recognition sites, especially through EGFR-based recognition sites. By this way, one is able to roughly distinguish normal lung and NSCLC cell-derived exosomes by the three recognition sites, thus speculating the types of normal lung and NSCLC cells.

3.5. Multiplex identification for parent cell types of NSCLC-derived exosomes

By following of successful determination for normal lung and NSCLC cell-derived exosomes by multiple recognition sites, we will try to identify different NSCLC cell line-derived exosomes by over-expressed proteins: CD63, EpCAM, and EGFR. First of all, A549, H1299, and H460 cell-derived exosomes were simultaneously injected into three channels of the flow cell. As expected, it is found that the SPRi signal responses by EGFR sites were largest among the three types of exosomes as shown in Fig. 5, suggesting that EGFR has a highest expression on these NSCLC-derived exosomes. However, the SPRi signal response of H1299 cell-derived exosomes by EpCAM sites was almost twice as intensive as those of A549 and H460 cell-derived exosomes (see Fig. 5D), which signifies that the abundance of EpCAM protein in NSCLC cell-derived exosomes varies in sequence: H1299 > A549 ≈ H460.

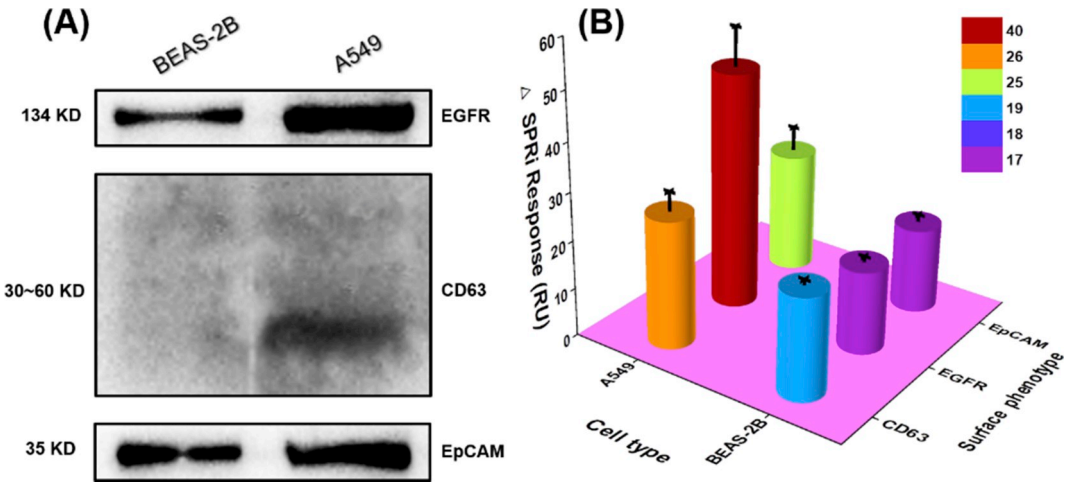

Fig. 4. Surface phenotype analysis of A549 cell-derived exosomes by Western blot and SPRi biosensor: (A) Western blot of A549 cell-derived exosomes, confirming CD63, EpCAM and EGFR on this exosome. And BEAS-2B cell-derived exosomes was used as reference; (B) SPRi signal responses from A549 and BEAS-2B cell-derived exosomes (130 μL of 4 × 10^5 particles/μL exosomes) through different recognition sites. All data were expressed as mean ± standard variation (n = 3).

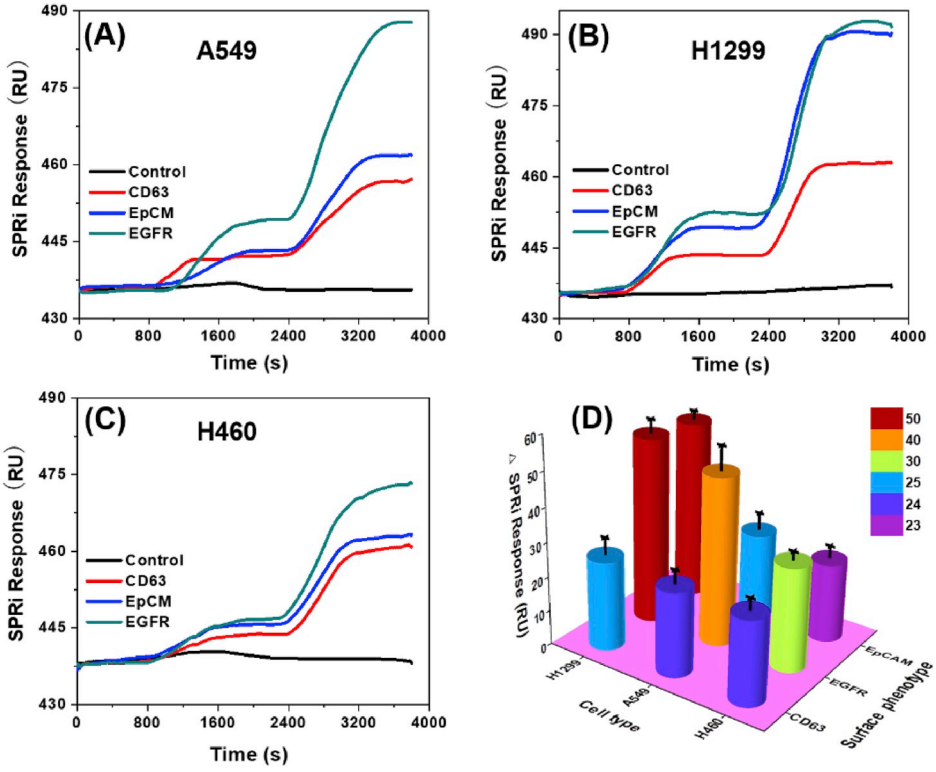

Fig. 5. SPRi sensorgrams for detecting NSCLC-related exosomes from: (A) A549; (B) H1299; and (C) H460 cell lines by CD63 (red), EpCAM (blue), and EGFR (green) sites, respectively; (D) Comparison of SPRi signal responses for NSCLC-related exosomes via different recognition sites. All data were expressed as mean ± standard variation (n = 3). (For interpretation of the references to color in this figure legend, the reader is referred to the Web version of this article.)

Nevertheless, SPRi signals of the three NSCLC cell-derived exosomes by CD63 sites, as one of the most typical protein in various exosomes, have almost equal of responses when these exosomes were added into flow chamber. Thus, it is speculated that the CD63 remained a moderate level and almost the same among the three kinds of NSCLC cell-derived exosomes (Im et al., 2014). Consequently, our constructed SPRi array has ability to analyze different NSCLC cell-derived exosomes and evaluate the abundance of over-expressed proteins, by which it has possibility to identify parent cell types of NSCLC-related exosomes and provide more assistance for diagnostic, monitoring and therapeutics.

3.6. Analysis of exosomes levels in clinical samples

To further validate utility of our developed SPRi array in clinical samples, we tested the NSCLC cell-derived exosomes based on the CD63 sites in plasma from healthy volunteers (normal group, denoted as H), the preliminary diagnostic NSCLC patients (NSCLC group, denoted as P), and NSCLC patients getting relief from treatment (treatment group, denoted as T), respectively. As shown in Fig. 6, the level of exosomes seemed to the highest in NSCLC patient group, but lower in the set of treatment group. Additionally, the exosomes' levels of normal group were the lowest among all of groups. Notably, more vesicles are secreted from NSCLC issues than normal to engage in malignant biological activity (Jakobsen et al., 2015). For the treatment group, the amounts of exosomes were between the NSCLC group and normal group, signifying the tumor extinction after therapies. Thus, this developed SPRi method demonstrates potential in not only distinguishing cancer patients from normal samples but also evaluating therapeutic efficacy by measuring abundance of exosomes from plasma.

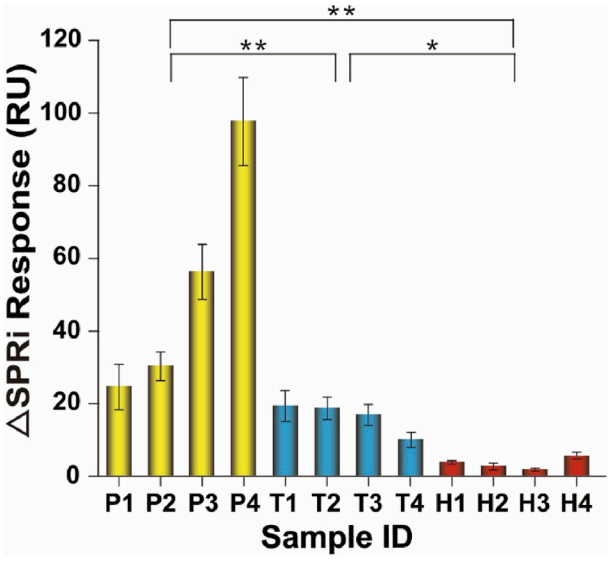

Fig. 6. Levels analysis of NSCLC-related exosomes (130 μL) from NSCLC, treated patients, and normal samples by the SPRi biosensing assay. A serial of archival plasma samples from NSCLC patients (yellow, P1∼P4), treated patients (blue, T1∼ T4), and healthy volunteers (red, H1∼ H4) were screened for levels of NSCLC-related exosomes, respectively. All data expressed as mean ± standard variation (n = 3). Significance was determined by Student unpaired *t*-test (*$p < 0.5$; **$p < 0.05$). (For interpretation of the references to color in this figure legend, the reader is referred to the Web version of this article.)

4. Conclusion

In summary, a novel SPRi-based biosensing assay was successfully developed for multiplex characterization of NSCLC-related exosomes by different recognition sites. Limit of detection (LOD) towards NSCLC-derived exosomes was estimated to be 2.37×10^4 particles/μL,

benefiting from the amplification of AuNPs. By this way, one is able to distinguish normal lung and NSCLC cell-derived exosomes through precise identification of the exosomal protein pattern. More importantly, the biosensing method is able to analyze different NSCLC cell-derived exosomes and evaluate the abundance of over-expressed proteins, by which it has possibility to identify parent cell types of NSCLC-related exosomes. Furthermore. the developed assay was successfully applied for the detection of exosomes from clinical samples. This biosensing strategy will be applicable of massive high-throughput screening for NSCLC in clinical specimens, offering the possibility for diagnosis of NSCLC and help in designing potential curative options. However, a disadvantage of the biosensing assay is the limitation of application in point-of-care test. And future work will focus on portable SPRi system construction and flexible method for exosomes purification.

Declaration of competing interest

The authors declare that they have no known competing financial interests or personal relationships that could have appeared to influence the work reported in this paper.

CRediT authorship contribution statement

Yunpeng Fan: Conceptualization, Methodology, Software, Investigation, Data curation, Writing - original draft, Project administration. **Xiaolei Duan:** Conceptualization, Methodology, Software, Investigation, Data curation, Writing - original draft, Project administration. **Min Zhao:** Software, Writing - original draft, Investigation. **Xiaotong Wei:** Methodology, Formal analysis, Software. **Jiangling Wu:** Methodology, Formal analysis, Software. **Wenqin Chen:** Conceptualization, Data curation. **Ping Liu:** Resources, Software. **Wei Cheng:** Resources, Validation. **Quan Cheng:** Resources, Validation. **Shijia Ding:** Supervision, Methodology, Data curation, Funding acquisition, Project administration, Data curation.

Acknowledgment

We are grateful for the financial support from the National Natural Science Foundation of China (81873980, 81873972, 21804015), the National Science and Technology Major Project of the Ministry of Science and Technology of China (2018ZX10732202), China Postdoctoral Science Foundation Funded Project (2017M622980), and Natural Science Foundation Project of CQ (cstc2018jcyjAX0201, cstc2018jcyjAX0251). X.D. acknowledges the Elite Person-time Training Project of Zunyi Medical College. We also thank professor Quan Cheng, from University of California, for his assistance in setting up the SPRi platform.

Appendix A. Supplementary data

Supplementary data to this article can be found online at https://doi.org/10.1016/j.bios.2020.112066.

References

Abbosh, C., Birkbak, N.J., Wilson, G.A., Jamal-Hanjani, M., Constantin, T., Salari, R., Le Quesne, J., Moore, D.A., Veeriah, S., Rosenthal, R., 2017. Nature 545 (7655), 446–451.
Aguiar Jr., P.N., Santoro, I.L., Tadokoro, H., de Lima Lopes, G., Filardi, B.A., Oliveira, P., Mountzios, G., De Mello, R.A., 2016. Immunotherapy 8 (4), 479–488.
Boriachek, K., Islam, M.N., Möller, A., Salomon, C., Nguyen, N.-T., Hossain, M.S.A., Yamauchi, Y., Shiddiky, M.J.A., 2018. Small 14 (6), 1702153.
Bray, F., Ferlay, J., Soerjomataram, I., Siegel, R.L., Torre, L.A., Jemal, A., 2018. CA Cancer J. Clin. 68 (6), 394–424.
Clark, D.J., Fondrie, W.E., Yang, A., Mao, L., 2016. J. Proteomics 133, 161–169.
Di Noto, G., Bugatti, A., Zendrini, A., Mazzoldi, E.L., Montanelli, A., Caimi, L., Rusnati, M., Ricotta, D., Bergese, P., 2016. Biosens. Bioelectron. 77, 518–524.
Ferhan, A.R., Jackman, J.A., Park, J.H., Cho, N.J., Kim, D.H., 2018. Adv. Drug Deliv. Rev. 125, 48–77.
Gool, E.L., Stojanovic, I., Schasfoort, R.B., Sturk, A., Van Leeuwen, T.G., Nieuwland, R., Terstappen, L.W., Coumans, F.A., 2017. Clin. Chem. 63 (10), 1633–1641.
He, M., Crow, J., Roth, M., Zeng, Y., Godwin, A.K., 2014. Lab Chip 14 (19), 3773–3780.
Herbst, R.S., Morgensztern, D., Boshoff, C., 2018. Nature 553 (7689), 446–454.
Ho, M.M., Ng, A.V., Lam, S., Hung, J.Y., 2007. Cancer Res. 67 (10), 4827–4833.
Im, H., Shao, H., Park, Y.I., Peterson, V.M., Castro, C.M., Weissleder, R., Lee, H., 2014. Nat. Biotechnol. 32 (5), 490.
Jakobsen, K.R., Paulsen, B.S., Bæk, R., Varming, K., Sorensen, B.S., Jørgensen, M.M., 2015. J. Extracell. Vesicles 4 (1), 26659.
Jiang, Y., Shi, M., Liu, Y., Wan, S., Cui, C., Zhang, L., Tan, W., 2017. Angew. Chem. Int. Ed. 56 (39), 11916–11920.
Kwizera, E.A., O'Connor, R., Vinduska, V., Williams, M., Butch, E.R., Snyder, S.E., Chen, X., Huang, X., 2018. Theranostics 8 (10), 2722–2738.
Li, T.-D., Zhang, R., Chen, H., Huang, Z.-P., Ye, X., Wang, H., Deng, A.-M., Kong, J.-L., 2018. Chem. Sci. 9 (24), 5372–5382.
Liu, C., Guo, J., Tian, F., Yang, N., Yan, F., Ding, Y., Wei, J., Hu, G., Nie, G., Sun, J., 2017. ACS Nano 11 (7), 6968–6976.
Lobb, R.J., van Amerongen, R., Wiegmans, A., Ham, S., Larsen, J.E., Möller, A., 2017. Int. J. Canc. 141 (3), 614–620.
Lv, S., Zhang, K., Zeng, Y., Tang, D., 2018. Anal. Chem. 90 (11), 7086–7093.
Lyon, L.A., Musick, M.D., Natan, M.J., 1998. Anal. Chem. 70 (24), 5177–5183.
Maltez-da Costa, M., de la Escosura-Muñiz, A., Nogués, C., Barrios, L., Ibáñez, E., Merkoçi, A., 2012. Nano Lett. 12 (8), 4164–4171.
Navab, R., Strumpf, D., Bandarchi, B., Zhu, C.-Q., Pintilie, M., Ramnarine, V.R., Ibrahimov, E., Radulovich, N., Leung, L., Barczyk, M., 2011. Proc. Natl. Acad. Sci. U. S.A. 108 (17), 7160–7165.
Oliveira-Rodriguez, M., Lopez-Cobo, S., Reyburn, H.T., Costa-Garcia, A., Lopez-Martin, S., Yanez-Mo, M., Cernuda-Morollon, E., Paschen, A., Vales-Gomez, M., Blanco-Lopez, M.C., 2016. J. Extracell. Vesicles 5, 31803.
Picciolini, S., Gualerzi, A., Vanna, R., Sguassero, A., Gramatica, F., Bedoni, M., Masserini, M., Morasso, C., 2018. Anal. Chem. 90 (15), 8873–8880.
Sandfeld-Paulsen, B., Jakobsen, K.R., Bæk, R., Folkersen, B.H., Rasmussen, T.R., Meldgaard, P., Varming, K., Jørgensen, M.M., Sorensen, B.S., 2016. J. Thorac. Oncol. 11 (10), 1701–1710.
Scarano, S., Mascini, M., Turner, A.P., Minunni, M., 2010. Biosens. Bioelectron. 25 (5), 957–966.
Shao, H., Im, H., Castro, C.M., Breakefield, X., Weissleder, R., Lee, H., 2018. Chem. Rev. 118 (4), 1917–1950.
Taverna, S., Giallombardo, M., Gil-Bazo, I., Carreca, A.P., Castiglia, M., Chacártegui, J., Araujo, A., Alessandro, R., Pauwels, P., Peeters, M., 2016. Oncotarget 7 (19), 28748–28760.
Thakur, A., Qiu, G., Ng, S.P., Guan, J., Yue, J., Lee, Y., Wu, C.L., 2017. Biosens. Bioelectron. 94, 400–407.
Van Niel, G., D'Angelo, G., Raposo, G., 2018. Nat. Rev. Mol. Cell Biol. 19 (4), 213–228.
Wang, N., Song, X., Liu, L., Niu, L., Wang, X., Song, X., Xie, L., 2018. Canc. Sci. 109 (5), 1701–1709.
Wu, X., Chen, H., Wang, X., 2012. Canc. Treat Rev. 38 (6), 580–588.
Yang, C.-H., Chou, H.-C., Fu, Y.-N., Yeh, C.-L., Cheng, H.-W., Chang, I.-C., Liu, K.-J., Chang, G.-C., Tsai, T.-F., Tsai, S.-F., 2015. Biochim. Biophys. Acta 1852 (7), 1540–1549.
Yu, X., He, L., Pentok, M., Yang, H., Yang, Y., Li, Z., He, N., Deng, Y., Li, S., Liu, T., 2019. Nanoscale 11 (33), 15589–15595.
Zeng, R., Luo, Z., Su, L., Zhang, L., Tang, D., Niessner, R., Knopp, D., 2019. Anal. Chem. 91 (3), 2447–2454.
Zhu, L., Wang, K., Cui, J., Liu, H., Bu, X., Ma, H., Wang, W., Gong, H., Lausted, C., Hood, L., 2014. Anal. Chem. 86 (17), 8857–8864.